

Risk factor identification for incident heart failure using neural network distillation and variable selection

Yikuan Li
yikuan.li@wrh.ox.ac.uk
Deep Medicine, University of Oxford

Shishir Rao
Mohammad Mamouei
Gholamreza Salimi-Khorshidi
Dexter Canoy
Abdelaali Hassaine
Thomas Lukasiewicz
Kazem Rahimi
Deep Medicine, University of Oxford

ABSTRACT

Recent evidence shows that deep learning models trained on electronic health records from millions of patients can deliver substantially more accurate predictions of risk compared to their statistical counterparts. While this provides an important opportunity for improving clinical decision-making, the lack of interpretability is a major barrier to the incorporation of these ‘black-box’ models in routine care, limiting their trustworthiness and preventing further hypothesis-testing investigations. In this study, we propose two methods, namely, model distillation and variable selection, to untangle hidden patterns learned by an established deep learning model (BEHRT) for risk association identification. Due to the clinical importance and diversity of heart failure as a phenotype, it was used to showcase the merits of the proposed methods. A cohort with 788,880 (8.3% incident heart failure) patients was considered for the study. Model distillation identified 598 and 379 diseases that were associated and dissociated with heart failure at the population level, respectively. While the associations were broadly consistent with prior knowledge, our method also highlighted several less appreciated links that are worth further investigation. In addition to these important population-level insights, we developed an approach to individual-level interpretation to take account of varying manifestation of heart failure in clinical practice. This was achieved through variable selection by detecting a minimal set of encounters that can maximally preserve the accuracy of prediction for individuals. Our proposed work provides a discovery-enabling tool to identify risk factors in both population and individual levels from a data-driven perspective. This helps to generate new hypotheses and guides further investigations on causal links.

KEYWORDS

risk factor, neural networks, electronic health records

1 INTRODUCTION

With the growing access to large-scale electronic health records (EHR) from millions of patients in recent years, deep learning provides an unprecedented opportunity to tackle risk prediction in a data-driven way [2, 10, 32]. Previous evidence demonstrated that deep learning models substantially outperform statistical models in terms of risk prediction [3, 6, 7, 18, 21, 27]. Nevertheless, due to their deep, complex architecture, it is difficult to retrieve medical

knowledge from these models for further clinical usage, hindering their wider applications in healthcare. Therefore, there is a need for further work on the interpretability of these models.

Current model interpretation methods mainly focus on the discovery of a subset of relevant features and the quantification of their importance for a particular task. Some of the commonly used methods are sequential correlation feature selection [12], mutual information feature selection [25], and Shapley values [33]. However, these methods can only discover important features from a number of fixed, pre-selected features, thus, are not flexible enough to untangle patterns learned from longitudinal EHR with various number of visits and records for each patient.

Heart failure (HF) is considered a major public health problem. Despite evidence indicating the decline in incidence and better survival rates, the prevalence of HF has been increasing [8, 31, 37]. Almost 920,000 people have been diagnosed with HF in the UK in 2018 [28] and the five-year mortality rate remained as high as approximately 50% [5, 9]. Therefore, identifying early-stage risk for HF to guide decision making is important. Statistical models have been used extensively for the prediction of incident HF risk and the identification of associative and causal factors of HF. Such studies have contributed to a better understanding of some the determinants of HF [1, 16, 17, 26]. For instance, 27 clinical factors have been verified to be associated with incident HF in 15 different studies [37]. However, on average, their predictive performance has been unsatisfactory, outlining omitted variables or inadequate modelling strategies [9, 22, 31].

In this study, we proposed two methods, namely, model distillation and variable selection, to interpret a state-of-the-art probabilistic sequential deep learning model, BEHRT [23], for HF risk association identification. To this end, BEHRT was trained on longitudinal linked EHR for the prediction of incident HF. Subsequently, we applied model distillation [13, 35] on BEHRT to extract the learned hidden patterns and incorporate them into a simpler, more interpretable model. In order to provide an uncertainty estimation for predictions as the probabilistic BEHRT model, we designed the model as a Bayesian deep learning model. The simple model was designed to combine the merits of two types of latent variables, namely, contextual variables and additive variables, for HF risk prediction. The contextual variable captured the complex temporal interactions of input features with the use of a bidirectional long short-term memory (BiLSTM) neural network. The additive

variable was constructed as the weighted sum of independent input features (with no interactions) where the weights provided an intuitive way to quantify the association of each feature to HF. The contextual variable and additive variable were then fed into a Gaussian processes (GP) classifier to produce a risk prediction that captured the two components. The motivation behind this design was to separate the additive elements of risk (as reflected by independent variables) from the elements that arise from more complex interactions between input features (captured by contextual variables). Before further investigation in interpretation and association identification, we validate the reliability of the model using area under receiver operating characteristic curve (AUROC) and area under precision-recall curve (AUPRC).

The identification of medical conditions that are associated or dissociated (i.e., negatively associated) with HF is carried out by analysing their contribution to the additive and the contextual variables. For the additive variable, the contribution of each condition to risk of HF is captured by the corresponding coefficient in the weighted sum. The contextual variable is a more abstract representation of nonlinear interactions between medical conditions over time, modelled by a BiLSTM. Therefore, we define the relative contextual variable risk of an event to HF as the ratio of the contextual variable in the event (e.g. diabetes, hypertension, or angina) exposure and non-exposure groups; similar to the notion of hazard ratio or relative risk in statistics. We mapped all diseases into an association map based on relative contextual variable and corresponding weight in additive variable (Section 3.4). This map directly reflected the population-level association between a disease and incident HF. In addition, to further support individual-level decision making, we conducted a variable selection method to maximally preserve a patient's temporal information while keeping as minimal critical records as possible. Therefore, with a much smaller number of records, the model can have a similar predictive performance as using the entire EHR. We present this as to give an overview of the structure of the paper.

2 METHODS

2.1 EHR dataset

Our dataset was acquired from Clinical Practice Research Datalink (CPRD) [29]. It includes records collected from general practices across the UK, and can be linked to hospital records and other secondary datasets such as the Office for National Statistics. To interpret the previously proposed BEHRT model for incident HF prediction, we followed the identical data pre-processing method in the original paper [23]. In brief, we used records between 1985 and 2015, for both men and women who were at least 16 years old. Clinical information included diagnoses, medications, and date of birth. All the diagnoses were mapped to the 10th revision of the International Statistical Classification of Diseases and Related Health Problems (ICD-10) [4] based on a previously published dictionary [23] and all medications were mapped to the British National Formulary (BNF) code in section level. Our dataset comprised 788,880 patients, 8.3% of whom were diagnosed with incident HF during the 6-months prediction window (HF +). We randomly split the dataset into a 60% training set, a 10% tuning set, and a 30% validation set.

2.2 Model performance evaluation

The direct interpretation of a complex model is challenging. This work aims to transfer the predictive capability from an established complex model to a simpler and more interpretable model using knowledge distillation to identify the associations that underlie the model's predictions. Therefore, the first concern would be the generalisability and predictive performance of the new model. In this analysis, we developed three models for comparison: an established probabilistic BEHRT as the reference model, a simple Bayesian deep learning model that distils knowledge from the BEHRT model, referred to as BDLD, and the same Bayesian deep learning model trained without distillation mechanism (referred to as BDL for simplicity) [20, 35]. The objective is to prove that with knowledge distillation, the simple BDLD model can achieve a comparable predictive performance and generalisability, therefore, it is a valid model that can be further used for the interpretation of risk associations.

All models were trained and tuned using training and tuning set, respectively. Afterwards, we evaluated these models on the validation set and compared their predictive performance using AUROC, AUPRC, and the calibration curve. Since all probabilistic models generated a probability distribution for the risk of HF, the mean and the confidence interval were calculated as follows: (1) a random sample of size 30 was drawn from the predicted probability distribution of a given patient, and all metrics were evaluated using the mean probability over these 30 samples; (2) a random sample of size 1 was drawn from the predicted probability distribution of a given patient, all metrics were calculated based on this sample, afterwards, this process was calculated for 30 times, and we reported the mean and 95% confidence interval over these 30 evaluations. The first method focused on evaluating a model's average predictive performance, and the second method can show the stability of model predictions. Also, we did not see any material difference when we sampled more than 30 times.

2.3 Model architectures

This study involved two model architectures (3 scenarios): A Transformer-based BEHRT model, a Bayesian deep learning model trained without knowledge distillation (BDL), and the same Bayesian deep learning model trained with model distillation (BDLD).

The BEHRT model is based on a recently proposed Transformer architecture [23], which uses attention mechanism to extract long-term dependencies within sequential data. It treats a medical event as word, a visit as sentence, and the entire EHR as a document to mimic how natural language processing models model the sequential language. Instead of building sequential dependencies event by event like recurrent neural network [39], it uses auxiliary features such as age, segmentation, positional code to represent the order, as well as the irregular interval between events. Additionally, the probabilistic BEHRT model uses stochastic embedding parameters and a Gaussian processes classifier for prediction. We refer readers to the original paper [23] for more details.

For the BDL(D) model, as shown in Figure 1, it included three components: a one-layer bidirectional long short-term memory network [38], a one-layer feed-forward network, and a Gaussian processes classifier [23, 36]. The BiLSTM component, in which the embedding parameters are stochastic, was designed to extract the

interactions of temporal features and summarise them as a contextual variable. The feed-forward network (weight parameters are stochastic) was equivalent to a linear component, which assigned a coefficient to each feature (predictor) to represent its association to prediction. Both risk scores are learned by the neural network. We summed the coefficient of events with occurrence in a patient's medical records as a single score (additive variable) to represent risk learned from independent predictors. In the end, we used a Gaussian processes classifier to learn a multivariate correlation among the contextual variable, additive variable, and risk of incident HF.

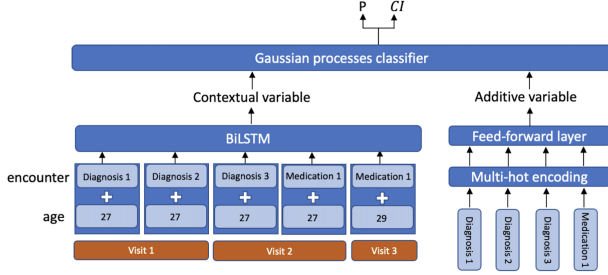


Figure 1: Bayesian deep learning model (BDL and BDLD) architecture. P represents the mean predictive probability; CI represents predictive 95% confidence interval. For BiLSTM, we feed the events in the EHR as a sequence, with age to represent their order. For the feed-forward layer, we encode the medical events into a multi-hot vector, where each dimension represents whether an event occurred in a patient's medical history. As shown, there are two medication 1 recorded in the patient's history, however, for a multi-hot encoder, we only need to feed in if medication 1 is recorded or not, while the number of repetitions is irrelevant.

2.4 Model distillation

Model distillation includes two components: a teacher network and a student network. The teacher network is a well-trained established deep learning model (BEHRT in our case), and the student network is a simpler model or a target model that we intend to use it to distil knowledge from the teacher network (BDLD in our case). Tang et al. [35] developed a strategy to train a student model with partial assistance from teacher models to help the student network achieve a competitive performance, and Korattikara et al. [20] proposed a Bayesian deep learning-based knowledge distillation method to transfer knowledge between probabilistic models. In this work, we combine both methods to use the probabilistic teacher network BEHRT to partially supervise the training of the probabilistic student network BDLD. As shown in Figure 2, both the teacher network and the student network use the same input information. Afterwards, the prediction from the teacher network will be used as a soft label to partially supervise the training of the student model. At the same time, the student model is also trying to predict the real label. Therefore, the loss function can be summarized as below:

$$L = \alpha \cdot L_{ELBO} + (1 - \alpha) \cdot L_{distill}, \quad (1)$$

where α represents a pre-set weight to balance the training objective for mimicking the teacher and leaning for the classification task. L_{ELBO} represents the loss for evidence lower bound, and $L_{distill}$ is the loss for knowledge distillation. We used cross entropy for negative log-likelihood in evidence lower bound. Additionally, the loss for knowledge distillation is shown as below:

$$L_{distill} = p(y|x, \theta^t) \log S(y|x, \omega) + (1 - p(y|x, \theta^t)) \log (1 - \log S(y|x, \omega)), \quad (2)$$

where $S(y|x, \omega)$ represents the outputs from the student network, $p(y|x, \theta^t)$ represents the outputs from the teacher network, θ^t are the parameters for the teacher network, and ω is the weights for student network. The distillation loss can also be considered as a reframing of the standard cross entropy loss.

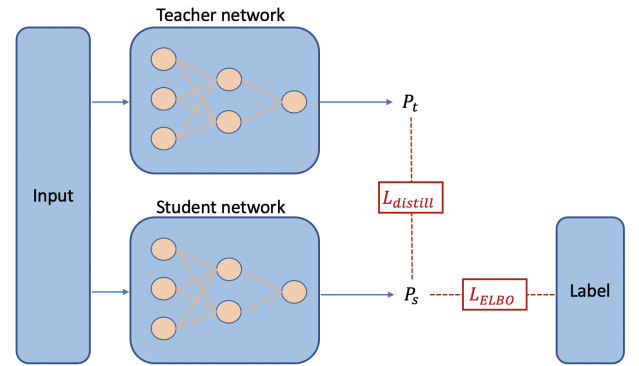


Figure 2: Illustration of model distillation. The figure shows the mechanism of model distillation. P_t and P_s represent a prediction sampled from the predictive distribution of the teacher network and the student network, respectively; $L_{distill}$ and L_{ELBO} are two loss functions for distillation and evidence lower bound, respectively.

2.5 Population-wise risk association analyses

The BDLD model decomposed the BEHRT model into two risk components: a contextual variable and an additive variable. The additive variable was the summation of coefficients of events that occurred in a patient's medical history, therefore, the coefficients directly reflected the association between the corresponding event and predicted risk.

$$Additive\ risk = \sum_{i=1}^E c_i \times e_i, \quad (3)$$

where c and e represent coefficient and event, respectively, and E represents events been considered by the multi-hot encoder.

For the contextual variable, we assumed a well-trained BDLD model that learned the population-wise pattern and can be used as a risk estimator to evaluate risk over population. Therefore, we assessed the association of an event (e.g., a disease or a medication) to HF by calculating the relative average contextual ratio between a group of patients without the exposure and a group of patients with the exposure similar to estimating the risk ratio in epidemiological

studies. We stratified the relative contextual ratio by age, and used the mean to represent the final relative contextual ratio. More details about age stratified calculation can be found in Appendix A.1.

$$CR = \frac{P(outcome|exposure = False)}{P(outcome|exposure = True)}, \quad (4)$$

where CR represents relative contextual ratio, $P(outcome|exposure = True/False) = \frac{1}{N} \sum_{i=1}^N P(outcome|exposure = True/False, C_i)$, N represents the number of patients in the exposure group and non-exposure group accordingly, and C_i represents the contextual information (records) for patient i . For each patient i , the risk P is the average contextual variable over 30 samples.

We used this approach to identify events, more specifically diseases, that were positively and negatively associated with HF.

2.6 Patient-wise feature selection

We proposed a novel patient-wise feature selection method to identify the most relevant event in a patient's medical history for his/her prediction. It used a parametrized Gumbel-softmax distribution to learn an importance score (between 0 to 1) of each event. Our method consisted of 2 networks: a baseline network and a predictor network. The baseline model was a well-trained BDL model and it predicts the risk using all medical records. We used such risk probability as reference to train the predictor model. For the predictor model, it was the same as the BDL model with all the weights fixed but with an importance-score layer (Figure 3). Our optimization objective was to preserve the predictive probability from the predictor network as close as possible to the predictive probability from the baseline model and keep the number of records with high importance score as minimal as possible. Therefore, our proposed method was capable of discovering the most relevant features to support risk prediction.

This approach took inspiration from the concept of a local surrogate model [24], which optimizes an independent interpreter for individual prediction. In order to detect the personalized association for incident HF prediction, we implemented an importance score vector that assigned a trainable variable to each record. Each variable of the importance score vector is ideally a Bernoulli distribution, representing whether a record is important for the prediction or not. However, Bernoulli distribution is not differentiable. Therefore, we used the Gumbel-Softmax distribution [14] as an estimator for the Bernoulli variables (between 0 and 1), which is proved to be an efficient training strategy for Bernoulli and categorical variables [14]. The training strategy is to optimize the trainable importance score to preserve a model's predictive capability while keeping as less important records as possible. We summarized this strategy into a loss function as below:

$$Loss = L_{prediction} + \gamma \cdot L_{anchor}, \quad (5)$$

$$L_{anchor} = SUM(\omega_{importance}), \quad (6)$$

$$L_{prediction} = MSE(P_b, P_p), \quad (7)$$

where $SUM(\omega_{importance})$ represents summation over Bernoulli variables (importance score) across events, MSE represents mean square error, and γ represents weight coefficient (usually between 0 and 1).

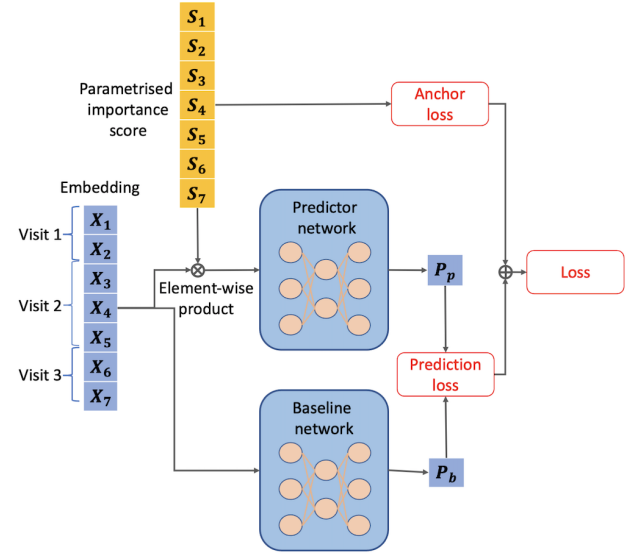


Figure 3: Block diagram of the patient-wise feature selection method. The figure shows the training mechanism for patient-wise feature selection. Embeddings, which are the summation of age and encounter embedding, are fed into both the baseline network and the predictor network. The baseline network thus provides a reference prediction P_b . Before feeding into the predictor network, the inputs are filtered with an importance score, therefore, it has a different prediction P_p . The objective is to minimise the summation of prediction loss and anchor loss.

2.7 Experimental setup

Models are implemented in PyTorch [30] and GPytorch [11]. We followed the parameters been set for the probabilistic BEHRT model [23] with maximum sequence length 256, hidden size 150, 4 layers of transformer, 6 attention heads, 108 intermediate hidden size, and 24 pooling size. We used 40 inducing points and radial basis function (RBF) kernel for the Gaussian processes classifier. For BDL(D), we used similar hyper parameters. Both encounter and age embeddings as well as hidden size for BiLSTM were 150, and 256 was set for the maximum sequence length. For those components that are stochastic and deployed following the Bayesian deep learning framework, we used the mean-field distribution to approximate the posterior. The normal distribution with 0 mean and 0.374 standard deviation was used as prior distribution for the weights of those components. For the sparse Gaussian processes classifier in the Bayesian deep learning model, we used 100 inducing points and the RBF kernel. We used $\alpha = 0.5$ for the model distillation training, and $\gamma = 0.1$ for patient-wise feature selection. The Adam [19] optimizer was used for both BEHRT and BDL(D). For BDL(D) in model distillation, we used the learning rate $7e^{-4}$ and batch size 256. The number of training epochs was governed by an early stopping strategy, and the training stopped when the loss did not improve after 5 epochs. For patient-wise feature selection, we used the learning rate $9e^{-2}$, and each sample was trained for 500 iterations.

3 RESULTS

3.1 Statistics for the risk prediction dataset

The characteristics of the patients in the training set, tuning set, and validation set, as well as in all patients are summarized in Table 1. All datasets were very similar with respect to demographics and statistics of the number of visits.

3.2 Model performance evaluation

We compared two models in three scenarios as described in Section 2.2: A Transformer-based probabilistic model, BEHRT, a proposed model with simpler architecture trained with knowledge distillation mechanism (i.e., BDLD), and the same simple model but trained without knowledge distillation (i.e., BDL).

The predictive performance of BEHRT, BDLD, and BDL on the validation set are shown in Figure 4. Figure 4A) exemplifies the probability distribution of developing HF, as predicted by the three models, for four randomly selected patients. In terms of average predictive probability (Figure 4B, C, D), BDLD achieved the best performance, and substantially outperformed the BDL model, reaching 0.94 and 0.63 for AUROC and AUPRC, respectively. It showed a comparable performance to BEHRT with a slight improvement (2%) in AUPRC. Additionally, BDLD also showed a better calibration than BEHRT. As similar pattern was observed when evaluating performance using mean with 95% confidence interval over 30 samples from the predictive distribution (Figure 4E, F, G). However, it is worth pointing out that the calibration curve in Figure 4G shows that BDLD preserved a similar uncertainty estimation pattern as BEHRT. Both of them indicated that the risk predictions at the higher end were more uncertain in our highly imbalanced dataset (with only 8.3% of positive samples).

In general, the model performance comparison illustrated that the proposed BDLD model achieved a similar performance to BEHRT despite its much simpler architecture. Moreover, BDLD preserved a similar uncertainty pattern as the BEHRT model, therefore, supporting its potential to replace the original BEHRT model for more down-stream risk association analysis.

3.3 Relation between latent variables and risk for BDLD

Our proposed BDLD model used a GP classifier to extract the multivariate correlation among contextual variables, additive variables, and predicted (HF) risk (Figure 1). The contextual variable captured the temporal interactions of input features using a BiLSTM, and the additive variable was the weighted sum of input features representing diagnoses and medication that ever occurred in a patient’s history. Both variables together indicated a patient’s risk of developing HF. Figure 5A and 5B show that the range of the contextual variable for HF (+) and HF (-) are approximately between -9.5 and -4, and the approximate range for the additive variable is between 7.5 to 9.5. We also see that the contextual variable is better at distinguishing between positive and negative cases while there remains substantial overlap when additive variables are considered, and combining both risk variables can lead to more reliable risk prediction (Figure 5C). We also need to clarify here that both variables are latent features learned by a neural network, and they are not

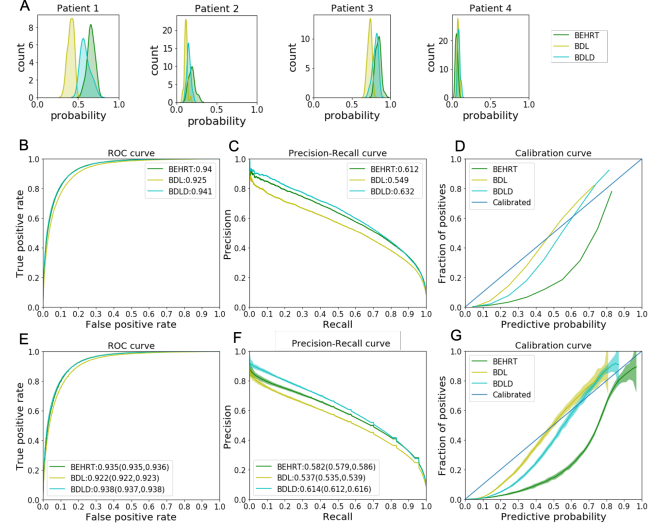


Figure 4: Performance evaluation of AI models on the validation set. BEHRT is an established incident HF risk prediction model, BDLD is our proposed Bayesian deep learning model trained with a distillation mechanism, and BDL is the same Bayesian deep learning model trained without distillation mechanism. A: Examples of predictions from four randomly selected patients, instead of predicting a single probability, all three models can present the predictive distribution, here, 30 samples are drawn from the predictive distribution for its approximation. B, C, D represent comparison of the ROC curve, precision-recall curve, and calibration curve among three models, all of them are conducted based on the mean predictive probability (i.e., average probability over 30 samples). E, F, G present the comparison of the ROC curve, precision-recall curve, and calibration curve by treating each sample separately, resulting in 30 sets of samples. Therefore, these figures can represent the uncertainty of the predictions with mean and 95% confidence interval.

numerically meaningful. We are more interested in understanding how these two variable groups relate to the risk of HF.

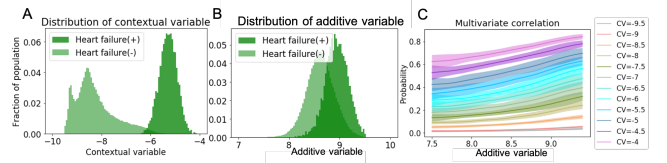


Figure 5: Analyses for multivariate correlation among contextual variable, additive variable, and predicted risk. A and B represent distribution of the contextual and additive variable, respectively. C is the multivariate correlation with the x axis represents additive variable, color represent contextual variable, and y axis represents the predictive distribution of HF risk

Table 1: Characteristics of patients

	All patients	Training set	Tuning set	Validation set
General characteristics				
No. of patients (% women)	788,880 (63)	473,394 (63)	78,900 (63)	236,586 (63)
No. of diagnosis code		1,533		
No. of medication code		360		
% White ethnicity (n)	43.8 (345,515)	43.8 (207,548)	43.8 (34,567)	43.7 (103,420)
% Unknown ethnicity (n)	42.6 (336,092)	42.6 (201,609)	42.6 (33,613)	42.6 (100,870)
Baseline characteristics				
Mean No. of visits per patient	84.9	85.0	84.9	84.8
Mean No. of codes per visit	2.02	2.02	2.02	2.02
Mean No. of diagnosis codes per visit	0.48	0.47	0.47	0.47
Mean (SD) follow-up (year)	8.9 (5.2)	8.9 (5.2)	8.9 (5.2)	8.9 (5.1)
Mean (SD) age (year)	57.1 (18.3)	57.1 (18.2)	57.1 (18.3)	57.1 (18.3)
SD: standard deviation				

By considering the range of contextual variables and additive variables simultaneously, Figure 5C further demonstrates the multivariate correlation between those two variables and the predicted risk. It shows that (1) the higher the value of the contextual variable and the higher the value of the additive variable, the higher the predicted risk, (2) high risk predictions have higher uncertainty than lower risk predictions, and (3) when the contextual variable is low (more towards -9.5), the prediction is extremely certain, and the additive variable does not provide much added value. We build on these trends as the basis of the population-wise association analysis in the next section.

3.4 Population-wise association analysis

By calculating the contextual ratio of the non-exposure group over the exposure group for diseases, along with their coefficients (additive variable is summation of coefficient of the diseases that occurred in a patient's medical records), we conducted analyses to identify population-wise risk associations (Figure 6). As previous analyses demonstrated, the higher the contextual variable and additive variable, the higher the predicted risk. Therefore, events (i.e., diseases) that have a higher contextual ratio and higher coefficient will have stronger associations with HF. Following this criterion, we identified 598 diseases with contextual ratio higher than 1 and coefficient higher than 0, indicating that they are potential associations. As shown in Figure 6, the upper left corner shows diseases with strong associations with HF, and most of them appear to be established risk factors, supporting the effectiveness of our proposed methods. Furthermore, we also identified 379 diseases that had a contextual ratio lower than 1 and a coefficient lower than 0, indicating potential dissociations. Although the signal for dissociations was weak (diseases do not have a low contextual ratio and low coefficient at the same time), comparing to the signal for associations, it is still worth pointing out that a few conditions such as 'noninflammatory disorders of uterus', 'lesion of plantar nerve', 'endometriosis', and 'excessive and frequent menstruation with regular cycle' indeed showed relatively strong dissociations with HF (suggesting that these conditions are associated with lower risk of

HF). We also included an age distribution analysis in Appendix B.1 for the identified dissociations to ensure they were conducted in a population with a reasonable age distribution rather than analyzing population with extreme cases. However, of course, these hypotheses require further confirmation in other studies or clinical trials. For diseases with contextual ratio higher than 1 and coefficient lower than 0 (lower left quadrant), the interpretation is unclear. One potential interpretation is that patients with those diseases indeed have a higher risk of developing HF, however, they have a far less direct association with HF, thus, increasing the uncertainty for the predicted risk. A similar assumption can also be applied to diseases with contextual ratio lower than 1 and coefficient higher than 0 (upper right quadrant). We also encourage readers to read the discussion in Appendix B.2 regarding potential concerns about correlation (or collinearity) among independent predictors.

3.5 Patient-wise association analysis

In many cases, especially when patients are highly heterogeneous, clinicians can be more interested in identifying patient-wise associations to support decision-making. Our proposed variable selection method to identify the importance score of each longitudinal record can untangle complex medical records and provide an interpretable explanation of the predictions made. As shown in Figure 7, we showcased two random examples and only a fraction of records is listed for illustration (full records can be found in Appendix B.3). Figure 7A and 7B firstly show that for both patients, only using a small fraction of key events (with high importance score), the model (BDLD) can achieve a similar predictive performance as using a patient's entire medical history. It supports the effectiveness of the identified key events. Furthermore, Figures 7C and 7D show a small fraction of records for both patients A and B. They demonstrate that the proposed method is very dynamic and can adapt to different patient scenarios to identify personalized key events depending on their context. We summarized the events with relatively high importance score for both patients A and B in Figures 7E and 7F, respectively. For patient A, we see that 'antiplatelet drugs', 'nitrate', 'calcium-channel blockers and other antianginal drugs', 'dyspepsia

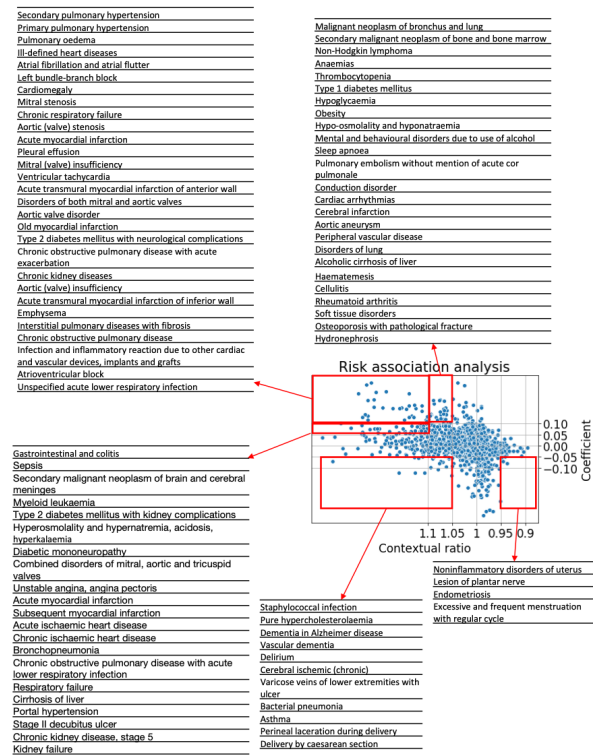


Figure 6: Risk factor association analysis. The x axis represents the contextual ratio and the y axis represent coefficient of diseases; the higher the contextual ratio and the higher the coefficient, the stronger the association between a disease and HF. The red boxes are randomly selected for visualization.

and gastro-oesophageal reflux disease', 'diuretics', and 'atrial fibrillation and atrial flutter' substantially contribute to the HF prediction. Because of the intensive repetition of 'diuretics' and most of its repetition are identified with a high importance score, we know 'diuretics' plays an important role for patient A. For patient B, a quite different pattern is identified. We see that 'antibacterial drugs', 'antihistamines, hypersensitisation and allergic emergencies', 'chronic obstructive pulmonary disease with acute exacerbation', 'diuretics', 'acute myocardial infarction', 'asthma', 'bronchodilators', and 'acute lower respiratory infection' are important key events that lead to the high risk prediction.

3.6 Discussion

Although deep learning models have been widely applied to various prognosis tasks and showed a superior predictive performance than the conventional statistical models, there still are major concerns about their explainability, which is becoming a major bottleneck that hinders the wider application of deep learning models for clinical usage and research. To tackle this difficulty, in this study, we provided a proof of concept that model distillation can be used as a discovery-enabling tool to identify population-wise potential risk

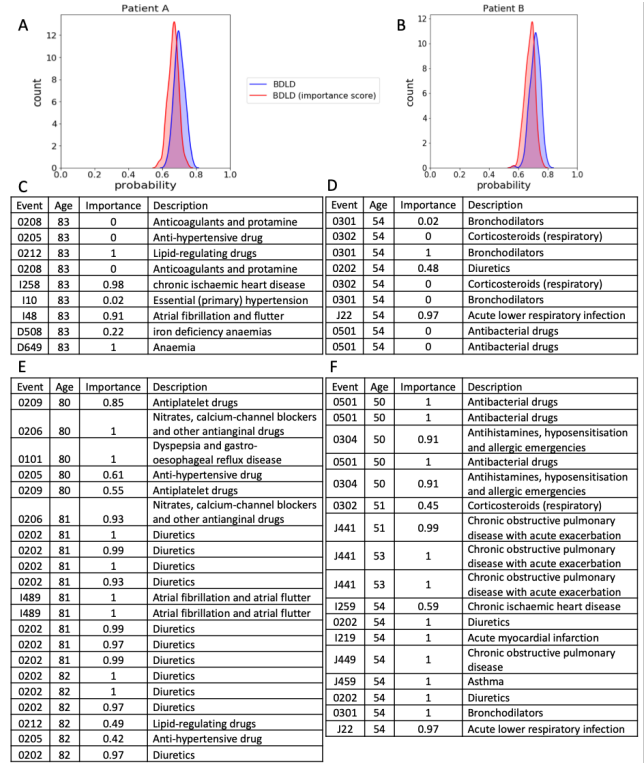


Figure 7: Patient-wise feature selection to identify associations and provide interpretable explanations of the predictions. Two patients are used for the illustration, with only a fraction of records been shown here. A and B represent the model predictive distributions for the model using full medical records, and a fraction of records with high importance score for patients A and B, respectively. C and D show a fraction of records for patients A and B. Event is event code, age is the age when corresponding event occurs, and the importance score is a trainable score between 0 and 1 to indicate the importance of the event, where 1 indicates high importance and 0 indicates low importance. E and F list events with relatively high importance score for patients A and B respectively.

factors for HF from a data-driven way without explicit expert engagement, and a variable selection analysis can accurately identify patient-wise associations to provide interpretable explanations to support trustworthiness of model predictions and decision-making. Although our work mainly focused on HF, the methodologies carried out from this work can be easily applied to other diseases of interest with minimal changes.

In this work, we introduced several methodological innovations for deep learning model interpretation. Firstly, instead of directly interpreting a deep and complex model (i.e., BEHRT), we used a model distillation mechanism to decompose the pattern learned by the deep model into two simpler components. One component represented the hidden interactions within the temporal trajectory, and the other component represented the risk of each disease or

medication to HF. We carefully designed these two components to be alike to the concept of interaction and independent predictor in the conventional statistical model for better interpretation. Despite the simple architecture of the distilled model, it was capable of achieving comparable or even better predictive performance than the BEHRT model, while preserving the uncertainty information which suggested that HF (+) predictions were more uncertain than HF (-) predictions in our highly imbalanced dataset.

Secondly, to untangle the risk of a disease in its temporal context, we combined the concept of relative risk and partial dependent plot [24], using the interaction component as an estimator and marginalizing the risk of patients over the exposure group and the non-exposure group to evaluate the relative risk of a disease. By using such a relative risk along with the learned coefficient of a disease, we managed to conduct an association map and saw that our findings were broadly consistent with prior knowledge of HF and corroborated risk factors of the disease. Our association map also raises questions that warrants further research. For instance, although there is some evidence from traditional epidemiological studies for an association between asthma and HF [34], this could not be supported in our study. Furthermore, as dissociation is a less well-established area in risk analysis, we surprisingly found potential dissociation between menstruation with regular cycle and HF aligned with the hypothesis of an on-going trial [15]. Therefore, our proposed method might be of great use to provide potential candidates for the investigation of factors that prevent a particular disease.

Thirdly, although population-wise risk association plays an important role in disease prevention, in practice, clinicians can be more interested in identifying critical events for individual patients to support decision-making. Our proposed variable selection method is designed to tackle this demand, showing a promising predictive performance even with only a small fraction of critical records. More specifically, we saw that using a subset of records with high importance score for prediction, the predictive distribution significantly aligned with the predictive distribution with all records, which proved the effectiveness of those key events. Additionally, our proposed variable selection method is very dynamic and can adapt to patients who are heterogeneous. For instance, in our results, we listed two patients who have different age and different trajectory (medical history). Our model indicated that ‘diuretics’ was an important signal for the older patient. Since diuretics are usually prescribed to patients who have symptoms of HF, it is reasonable that the model identifies it as a predictor. However, for the other younger patient, more diverse signals are captured. It shows a combination of chronic obstructive pulmonary disease with acute exacerbation, diuretics, acute myocardial infarction, asthma, bronchodilators, and acute lower respiratory infection in this patient’s recent history renders the patient high risk. By simplifying the medical records and emphasising the most important events, this proposed tool can greatly untangle the complexity of EHR and provide evidence to support prediction and aid clinical decision making, in particular when disease phenotypes are heterogeneous.

In general, we believe our proposed methods have a number of implications. First, model distillation can significantly prune the model and reduce model complexity, yet preserve the deep, complex model’s predictive capability. Thus, the deep learning

model can be easily deployed to various scenarios (e.g., limited computational and storage capacity, low latency) to aid decision-making process. For instance, the small model can be deployed on a local clinical environment or smart phone where computational resources are limited. Because of the accessibility of the model, it can be used to alert clinicians and even patients themselves for a presentative check when their longitudinal medical records are available. Secondly, our distillation model can distil the knowledge learned by a complex deep learning model into a simple model. By interpreting the contextual and independent pattern, it can provide a data-driven perspective to rapidly identify risk factors in both population and individual level without explicit engagement from experts.

Our work also has limitations. First, we only used limited modalities (diagnoses, medications, and age) for modelling. By incorporating more available information from EHR, we can potentially improve the predictive performance for HF prediction, leading to more accurate measurement for contextualised dependencies and providing a calibrated measurement for independent associations. Moreover, we only tested our methods on one EHR; all conclusions highly depend on our dataset. Therefore, further research must be pursued regarding transferability to other datasets.

REFERENCES

- [1] Sunil K Agarwal, Lloyd E Chambless, Christie M Ballantyne, Brad Astor, Alain G Bertoni, Patricia P Chang, Aaron R Folsom, Max He, Ron C Hoogeveen, Hanyu Ni, et al. 2012. Prediction of Incident Heart Failure in General Practice The Atherosclerosis Risk in Communities (ARIC) Study. *Circulation: Heart Failure* 5, 4 (2012), 422–429.
- [2] Jose Roberto Ayala Solares, Francesca Elisa Diletta Raimondi, Yajie Zhu, Fatemeh Rahimian, Dexter Canoy, Jenny Tran, Ana Catarina Pinho Gomes, Amir H. Payberah, Mariagrazia Zottoli, Milad Nazarzadeh, Nathalie Conrad, Kazem Rahimi, and Gholamreza Salimi-Khorshidi. 2020. Deep learning for electronic health records: A comparative review of multiple deep neural architectures. *Journal of Biomedical Informatics* 101 (2020), 103337. <https://doi.org/10.1016/j.jbi.2019.103337>
- [3] Brett K Beaulieu-Jones, Casey S Greene, et al. 2016. Semi-supervised learning of the electronic health record for phenotype stratification. *Journal of biomedical informatics* 64 (2016), 168–178.
- [4] Gerlind R Brämer. 1988. International statistical classification of diseases and related health problems. Tenth revision. *World health statistics quarterly. Rapport trimestriel de statistiques sanitaires mondiales* 41, 1 (1988), 32–36.
- [5] Javed Butler, Andreas Kalogeropoulos, Vasiliki Georgiopoulos, Rhonda Belue, Nicolas Rodondi, Melissa Garcia, Douglas C Bauer, Suzanne Satterfield, Andrew L Smith, Viola Vaccarino, et al. 2008. Incident heart failure prediction in the elderly: the health ABC heart failure score. *Circulation: Heart Failure* 1, 2 (2008), 125–133.
- [6] Edward Choi, Mohammad Taha Bahadori, Andy Schuetz, Walter F. Stewart, and Jimeng Sun. 2016. Doctor AI: Predicting Clinical Events via Recurrent Neural Networks. arXiv:1511.05942 [cs.LG]
- [7] Edward Choi, Mohammad Taha Bahadori, Jimeng Sun, Joshua Kulas, Andy Schuetz, and Walter Stewart. 2016. RETAIN: An Interpretable Predictive Model for Healthcare using Reverse Time Attention Mechanism. *Advances in neural information processing systems* 29 (2016), 3504–3512.
- [8] Shannon M Dunlay and Véronique L Roger. 2014. Understanding the epidemic of heart failure: past, present, and future. *Current heart failure reports* 11, 4 (2014), 404–415.
- [9] Justin B Echouffo-Tcheugui, Stephen J Greene, Lampros Papadimitriou, Faiez Zannad, Clyde W Yancy, Mihai Gheorghiade, and Javed Butler. 2015. Population Risk Prediction Models for Incident Heart Failure: A Systematic Review. *Circulation: Heart Failure* 8, 3 (2015), 438–447.
- [10] Pawan Singh Gangwar and Yasha Hasija. 2020. Deep Learning for Analysis of Electronic Health Records (EHR). In *Deep Learning Techniques for Biomedical and Health Informatics*. Springer, 149–166.
- [11] Jacob R. Gardner, Geoff Pleiss, David Bindel, Kilian Q. Weinberger, and Andrew Gordon Wilson. 2019. GPyTorch: Blackbox Matrix-Matrix Gaussian Process Inference with GPU Acceleration. arXiv:1809.11165 [cs.LG]
- [12] Mark Andrew Hall. 1999. Correlation-based Feature Selection for Machine Learning. (1999).

- [13] Geoffrey Hinton, Oriol Vinyals, and Jeff Dean. 2015. Distilling the Knowledge in a Neural Network. arXiv:1503.02531 [stat.ML]
- [14] Eric Jang, Shixiang Gu, and Ben Poole. 2017. Categorical Reparameterization with Gumbel-Softmax. arXiv:1611.01144 [stat.ML]
- [15] Jeffrey Jensen. 2012. *Relationship Between the Menstrual Cycle and Heart Disease in Women*. Retrieved January 4, 2020 from <https://clinicaltrials.gov/ct2/show/NCT01546454>
- [16] Andreas Kalogeropoulos, Vasiliki Georgiopolou, Bruce M Psaty, Nicolas Rodondi, Andrew L Smith, David G Harrison, Yongmei Liu, Udo Hoffmann, Douglas C Bauer, Anne B Newman, et al. 2010. Inflammatory markers and incident heart failure risk in older adults: the Health ABC (Health, Aging, and Body Composition) study. *Journal of the American College of Cardiology* 55, 19 (2010), 2129–2137.
- [17] William B Kannel, Ralph B D'Agostino, Halit Silbershatz, Albert J Belanger, Peter WF Wilson, and Daniel Levy. 1999. Profile for Estimating Risk of Heart Failure. *Archives of internal medicine* 159, 11 (1999), 1197–1204.
- [18] Woo Jung Kim, Ji Min Sung, David Sung, Myeong-Hun Chae, Suk Kyoan An, Kee Namkoong, Eun Lee, and Hyuk-Jae Chang. 2019. Cox Proportional Hazard Regression Versus a Deep Learning Algorithm in the Prediction of Dementia: An Analysis Based on Periodic Health Examination. *JMIR medical informatics* 7, 3 (2019), e13139.
- [19] Diederik P. Kingma and Jimmy Ba. 2017. Adam: A Method for Stochastic Optimization. arXiv:1412.6980 [cs.LG]
- [20] Anoop Korattikara Balan, Vivek Rathod, Kevin P Murphy, and Max Welling. 2015. Bayesian Dark Knowledge. *Advances in Neural Information Processing Systems* 28 (2015), 3438–3446.
- [21] Bum Chul Kwon, Min-Je Choi, Joanne Taery Kim, Edward Choi, Young Bin Kim, Soonwook Kwon, Jimeng Sun, and Jaegul Choo. 2019. RetainVis: Visual Analytics with Interpretable and Interactive Recurrent Neural Networks on Electronic Medical Records. *IEEE Transactions on Visualization and Computer Graphics* 25, 1 (Jan 2019), 299–309. <https://doi.org/10.1109/tvcg.2018.2865027>
- [22] Wayne C Levy and Inder S Anand. 2014. Heart Failure Risk Prediction Models: What Have We Learned?
- [23] Yikuan Li, Shishir Rao, Abdelaali Hassaine, Rema Ramakrishnan, Yajie Zhu, Dexter Canoy, Gholamreza Salimi-Khorshidi, Thomas Lukasiewicz, and Kazem Rahimi. 2020. Deep Bayesian Gaussian Processes for Uncertainty Estimation in Electronic Health Records. arXiv:2003.10170 [cs.LG]
- [24] Christoph Molnar. 2021. *Interpretable Machine Learning*. Retrieved January 4, 2020 from <https://christophm.github.io/interpretable-ml-book/>
- [25] Arpita Nagpal and Vijendra Singh. 2018. A Feature Selection Algorithm Based on Qualitative Mutual Information for Cancer Microarray Data. *Procedia computer science* 132 (2018), 244–252.
- [26] Vijay Nambi, Xiaoxi Liu, Lloyd E Chambless, James A De Lemos, Salim S Virani, Sunil Agarwal, Eric Boerwinkle, Ron C Hoogeveen, David Aguilar, Brad C Astor, et al. 2013. Troponin T and N-Terminal Pro-B-Type Natriuretic Peptide: a Biomarker Approach to Predict Heart Failure Risk—The Atherosclerosis Risk in Communities Study. *Clinical chemistry* 59, 12 (2013), 1802–1810.
- [27] P. Nguyen, T. Tran, N. Wickramasinghe, and S. Venkatesh. 2017. Deepr: A Convolutional Net for Medical Records. *IEEE Journal of Biomedical and Health Informatics* 21, 1 (2017), 22–30. <https://doi.org/10.1109/JBHI.2016.2633963>
- [28] National Institute of Health and Care Excellence (NICE). 2018. *Chronic heart failure in adults: diagnosis and management*. Retrieved January 4, 2020 from www.nice.org.uk/guidance/ng106
- [29] National Institute of Health Research, Medicines, and Healthcare products Regulatory Agency. 2020. *Clinical Practice Research Datalink (CPRD)*. Retrieved January 4, 2020 from <https://www.cprd.com>
- [30] Adam Paszke, Sam Gross, Francisco Massa, Adam Lerer, James Bradbury, Gregory Chanan, Trevor Killeen, Zeming Lin, Natalia Gimelshein, Luca Antiga, Alban Desmaison, Andreas Kopf, Edward Yang, Zachary DeVito, Martin Raison, Alykhan Tejani, Sasank Chilamkurthy, Benoit Steiner, Lu Fang, Junjie Bai, and Soumith Chintala. 2019. PyTorch: An Imperative Style, High-Performance Deep Learning Library. In *Advances in Neural Information Processing Systems* 32, H. Wallach, H. Larochelle, A. Beygelzimer, F. d'Alché-Buc, E. Fox, and R. Garnett (Eds.). Curran Associates, Inc., 8024–8035. <http://papers.neurips.cc/paper/9015-pytorch-an-imperative-style-high-performance-deep-learning-library.pdf>
- [31] Berhe W Sahle, Alice J Owen, Ken Lee Chin, and Christopher M Reid. 2017. Risk Prediction Models for Incident Heart Failure: A Systematic Review of Methodology and Model Performance. *Journal of Cardiac Failure* 23, 9 (2017), 680–687.
- [32] Benjamin Shickel, Patrick James Tighe, Azra Bihorac, and Parisa Rashidi. 2017. Deep EHR: A Survey of Recent Advances in Deep Learning Techniques for Electronic Health Record (EHR) Analysis. *IEEE journal of biomedical and health informatics* 22, 5 (2017), 1589–1604.
- [33] Erik Strumbelj and Igor Kononenko. 2014. Explaining prediction models and individual predictions with feature contributions. *Knowledge and information systems* 41, 3 (2014), 647–665.
- [34] Dianjianyi Sun, Tiange Wang, Yoriko Heianza, Jun Lv, Liyuan Han, Felicia Rabito, Tanika Kelly, Shengxu Li, Jiang He, Lydia Bazzano, et al. 2017. A History of Asthma From Childhood and Left Ventricular Mass in Asymptomatic Young Adults: The Bogalusa Heart Study. *JACC: Heart Failure* 5, 7 (2017), 497–504.
- [35] Raphael Tang, Yao Lu, Linqing Liu, Lili Mou, Olga Vechtomova, and Jimmy Lin. 2019. Distilling Task-Specific Knowledge from BERT into Simple Neural Networks. arXiv:1903.12136 [cs.CL]
- [36] Andrew Gordon Wilson, Zhiting Hu, Ruslan Salakhutdinov, and Eric P. Xing. 2016. Deep Kernel Learning. In *Proceedings of the 19th International Conference on Artificial Intelligence and Statistics (Proceedings of Machine Learning Research, Vol. 51)*, Arthur Gretton and Christian C. Robert (Eds.). PMLR, Cadiz, Spain, 370–378. <http://proceedings.mlr.press/v51/wilson16.html>
- [37] Hong Yang, Kazuaki Negishi, Petr Otahal, and Thomas H Marwick. 2015. Clinical prediction of incident heart failure risk: a systematic review and meta-analysis. *Open heart* 2, 1 (2015).
- [38] Shu Zhang, Dequan Zheng, Xinchun Hu, and Ming Yang. 2015. Bidirectional Long Short-Term Memory Networks for Relation Classification. In *Proceedings of the 29th Pacific Asia conference on language, information and computation*. 73–78.
- [39] Tehseen Zia and Usman Zahid. 2019. Long short-term memory recurrent neural network architectures for Urdu acoustic modeling. *International Journal of Speech Technology* 22, 1 (2019), 21–30.

A RESEARCH METHODS

A.1 Age stratified relative contextual risk analyses

To ensure the fairness for the calculation of risk ratio, we carefully conducted an age-stratified subgroup selection. For each disease, we grouped patients based on their age of the first incidence and their baseline age. The age groups that we considered were 45-55, 55-60, 60-65, 65-70, 70-75, 75-80, 80-85, and 85-90. For example, if diabetes is our interest, we will choose patients who have the incidence of diabetes between 45-55 (e.g., 46) and baseline between 45-55 (e.g., 54) in the exposure group, and choose patients who have never been diagnosed with diabetes before baseline age (between 45-55, e.g. 54) in the non-exposure group. We repeated this estimation for 45-55/55-60 (incident age/baseline age), 45-55/60-65, 45-55/65-70, 45-55/70-75 and other possible combinations, we ignored any group pair if there are no patients in either exposure group or non-exposure group. In the end, we used the mean over all age groups as the summarized single value to represent a disease's relative contextual ratio.



Figure 8: Baseline age distribution of exposure group and non-exposure group for diseases with disassociation. The left column represents age distribution for patients in the exposure group, the middle column represents age distribution of female patients in the non-exposure group, and the right column represents age distribution of male patients in the non-exposure group. PDF represents probability density function.

B SUPPLEMENTARY RESULTS

B.1 Age distribution analysis for diseases with disassociation

As shown in Figure 8, we see for all four diseases that are identified as disassociations, the distribution of baseline age in exposure group in general covers a quite wide range of ages with median between 40 to 60. Since we stratified our association analysis by age and the exposure groups are not extreme cases, the conclusion from our association analysis should be valid.

B.2 Discussion about correlation among independent predictors

The distilled-model used a one-layer feed-forward network (linear component) to learn the coefficient of each event. To address the concern for feature correlation, we randomly sampled 100,000 patients in the training set to calculate the Cramér's correlation between each feature pair. Among 1,898 events, only 19 pairs have correlation higher than 0.6 (Table 2). Additionally, considering we used variational inference with standard Gaussian prior for the weight training, which equals to adding L2-normal regulariser to penalise the training process, we would not worry about the feature correlation problem.

Table 2: Cramér's correlation for disease/medication pair with correlation higher than 0.6

Event A	Event B	Correlation
D57.0	D57.1	0.70
B37.3	N77.1	0.94
L40.5	M07.3	0.92
M51.1	G55.1	0.82
C15.9	C15.5	0.60
0106/0704/1002	G70.0	0.75
0602/6407	E05.9	0.68
7408	7411	0.60
7109	7408	0.60
7409	7408	0.79
1306	L70.0	0.62
1305	L40.9	0.62
1103	H10.3	0.63
7154	7119	0.75
1106	H40.9	0.60
0602	E03.9	0.74
0601	E11.9	0.63
0601	7119	0.64
0601	7154	0.71

B.3 Patient-wise association identification

Here, we list the full records for two random selected patients (i.e., Patient A and B) with the importance scores. Patients A and B are shown in Tables 3 and 4, respectively.

Table 3: Patient A

Code	Age	Score	Description	0101	81	0	Dyspepsia and gastro-oesophageal reflux disease
0212	80	0	Lipid-regulating drugs	0205	81	0	Anti-hypertensive drug
0212	80	0	Lipid-regulating drugs	0209	81	0	Antiplatelet drugs
0209	80	0.85	Antiplatelet drugs	0212	81	0	Lipid-regulating drugs
0206	80	1	Nitrates, calcium-channel blockers and other antianginal drugs	0206	81	0.93	Nitrates, calcium-channel blockers and other antianginal drugs
0101	80	1	Dyspepsia and gastro-oesophageal reflux disease	0202	81	1	Diuretics
0205	80	0.61	Anti-hypertensive drug	0206	81	0	Nitrates, calcium-channel blockers and other antianginal drugs
0209	80	0.55	Antiplatelet drugs	0205	81	0.37	Anti-hypertensive drug
0212	80	0.05	Lipid-regulating drugs	0101	81	0	Dyspepsia and gastro-oesophageal reflux disease
0205	80	0	Anti-hypertensive drug	0209	81	0	Antiplatelet drugs
0101	80	0.01	Dyspepsia and gastro-oesophageal reflux disease	0202	81	1	Diuretics
0206	80	0	Nitrates, calcium-channel blockers and other antianginal drugs	0212	81	0	Lipid-regulating drugs
0101	81	0	Dyspepsia and gastro-oesophageal reflux disease	0101	81	0	Dyspepsia and gastro-oesophageal reflux disease
0212	81	0	Lipid-regulating drugs	0205	81	0	Anti-hypertensive drug
0209	81	0	Antiplatelet drugs	0206	81	0	Nitrates, calcium-channel blockers and other antianginal drugs
0206	81	0	Nitrates, calcium-channel blockers and other antianginal drugs	0209	81	0	Antiplatelet drugs
0205	81	0.05	Anti-hypertensive drug	0212	81	0.01	Lipid-regulating drugs
J220	81	0.01	Acute lower respiratory infection	0202	81	0.01	Diuretics
0501	81	0	Antibacterial drugs	0209	81	0	Antiplatelet drugs
0209	81	0.08	Antiplatelet drugs	0206	81	0	Nitrates, calcium-channel blockers and other antianginal drugs
0205	81	0	Anti-hypertensive drug	0212	81	0	Lipid-regulating drugs
0101	81	0	Dyspepsia and gastro-oesophageal reflux disease	0202	81	0.99	Diuretics
0206	81	0	Nitrates, calcium-channel blockers and other antianginal drugs	0101	81	0	Dyspepsia and gastro-oesophageal reflux disease
0212	81	0	Lipid-regulating drugs	0205	81	0	Anti-hypertensive drug
J220	81	0	Acute lower respiratory infection	0106	81	0	Laxatives
0501/0504/1306	81	0	Antibacterial drugs/Antiprotozoal drugs/Acne and rosacea	0101	81	0	Dyspepsia and gastro-oesophageal reflux disease
0212	81	0	Lipid-regulating drugs	0212	81	0	Lipid-regulating drugs
0209	81	0	Antiplatelet drugs	0206	81	0	Nitrates, calcium-channel blockers and other antianginal drugs
0206	81	0	Nitrates, calcium-channel blockers and other antianginal drugs	0205	81	0	Anti-hypertensive drug
0101	81	0	Dyspepsia and gastro-oesophageal reflux disease	0202	81	1	Diuretics
0205	81	0	Anti-hypertensive drug	0209	81	0	Antiplatelet drugs
0501/0504/1306	81	0	Antibacterial drugs/Antiprotozoal drugs/Acne and rosacea	0212	81	0	Lipid-regulating drugs
0205	81	0.01	Anti-hypertensive drug	0205	81	0	Anti-hypertensive drug
0212	81	0	Lipid-regulating drugs	0202	81	0.93	Diuretics
0101	81	0	Dyspepsia and gastro-oesophageal reflux disease	I489	81	1	Atrial fibrillation and atrial flutter
0209	81	0	Antiplatelet drugs	I489	81	1	Atrial fibrillation and atrial flutter
0206	81	0	Nitrates, calcium-channel blockers and other antianginal drugs	0202	81	0.99	Diuretics
				0101	81	0	Dyspepsia and gastro-oesophageal reflux disease
				0212	81	0	Lipid-regulating drugs
				0208	81	0	Anticoagulants and protamine
				0205	81	0	Anti-hypertensive drug
				0212	81	0	Lipid-regulating drugs

0205	81	0	Anti-hypertensive drug	0106	82	0	Laxatives
0208	81	0	Anticoagulants and protamine	0212	82	0	Lipid-regulating drugs
0202	81	0.97	Diuretics	0202	82	1	Diuretics
0206	81	0	Nitrates, calcium-channel blockers and other antianginal drugs	0208	82	0	Anticoagulants and protamine
0208	81	0	Anticoagulants and protamine	0208	82	0	Anticoagulants and protamine
0101	81	0	Dyspepsia and gastro-oesophageal reflux disease	0212	82	0	Lipid-regulating drugs
0205	81	0	Anti-hypertensive drug	0205	82	0.42	Anti-hypertensive drug
0212	81	0	Lipid-regulating drugs	0202	82	0.97	Diuretics
0205	81	0	Anti-hypertensive drug	0208	82	0	Anticoagulants and protamine
0212	81	0	Lipid-regulating drugs	0212	82	0	Lipid-regulating drugs
0208	81	0	Anticoagulants and protamine	0205	82	0	Anti-hypertensive drug
0202	81	0.99	Diuretics	0208	82	0	Anticoagulants and protamine
0101	81	0	Dyspepsia and gastro-oesophageal reflux disease	0212	82	0	Lipid-regulating drugs
0202	82	0.98	Diuretics	0202	82	0.31	Diuretics
0212	82	0	Lipid-regulating drugs	0205	82	0	Anti-hypertensive drug
0101	82	0	Dyspepsia and gastro-oesophageal reflux disease	0208	82	0	Anticoagulants and protamine
0205	82	0	Anti-hypertensive drug	0212	82	0	Lipid-regulating drugs
0208	82	0	Anticoagulants and protamine	0202	82	0	Diuretics
0212	82	0	Lipid-regulating drugs	0205	82	0	Anti-hypertensive drug
0101	82	0	Dyspepsia and gastro-oesophageal reflux disease	0202	82	1	Diuretics
0208	82	0	Anticoagulants and protamine	0212	82	0	Lipid-regulating drugs
0205	82	0	Anti-hypertensive drug	0208	82	0	Anticoagulants and protamine
0202	82	1	Diuretics	0205	82	0	Anti-hypertensive drug
0208	82	0	Anticoagulants and protamine	0205	83	1	Anti-hypertensive drug
0212	82	0	Lipid-regulating drugs	0212	83	0	Lipid-regulating drugs
0205	82	0	Anti-hypertensive drug	0208	83	0	Anticoagulants and protamine
0202	82	1	Diuretics	0106	83	0	Laxatives
0206	82	0	Nitrates, calcium-channel blockers and other antianginal drugs	K590	83	0	Constipation
0101	82	0	Dyspepsia and gastro-oesophageal reflux disease	0205	83	0	Anti-hypertensive drug
I340	82	0.04	Mitral (valve) insufficiency	0206	83	0.01	Nitrates, calcium-channel blockers and other antianginal drugs
0208	82	0	Anticoagulants and protamine	0202	83	1	Diuretics
0205	82	0	Anti-hypertensive drug	0212	83	0.02	Lipid-regulating drugs
0212	82	0	Lipid-regulating drugs	0208	83	0	Anticoagulants and protamine
0206	82	0	Nitrates, calcium-channel blockers and other antianginal drugs	0101	83	0	Dyspepsia and gastro-oesophageal reflux disease
0205	82	0	Anti-hypertensive drug	0101	83	0	Dyspepsia and gastro-oesophageal reflux disease
0208	82	0	Anticoagulants and protamine	0202	83	1	Diuretics
0212	82	0	Lipid-regulating drugs	0206	83	0	Nitrates, calcium-channel blockers and other antianginal drugs
0202	82	0.97	Diuretics	0208	83	0.02	Anticoagulants and protamine
0212	82	0.49	Lipid-regulating drugs	0212	83	0	Lipid-regulating drugs
0202	82	0	Diuretics	0205	83	0	Anti-hypertensive drug
0205	82	0	Anti-hypertensive drug	K590	83	0.14	Constipation
0101	82	0	Dyspepsia and gastro-oesophageal reflux disease	0106	83	0	Laxatives
0208	82	0	Anticoagulants and protamine	0208	83	0	Anticoagulants and protamine
K590	82	0	Constipation	0205	83	0.01	Anti-hypertensive drug
				0206	83	0.01	Nitrates, calcium-channel blockers and other antianginal drugs
				0202	83	0.98	Diuretics
				0212	83	0.03	Lipid-regulating drugs
				0205	83	1	Anti-hypertensive drug

Code	Age	Score	Description
J441	50	0.1	Chronic obstructive pulmonary disease with acute exacerbation
0304	50	0	Antihistamines, hyposensitisation and allergic emergencies
J301	50	0.04	Allergic rhinitis due to pollen
0105/0302/	50	0.01	Chronic bowel disorders/Corticosteroids (respiratory)/
0501/0504/			Antibacterial drugs/Antiprotozoal drugs/
0603/0802/			Corticosteroids (endocrine)/Drugs affecting the immune response/
1001			Drugs used in rheumatic diseases and gout

Code	Age	Score	Description
J441	50	0.1	Chronic obstructive pulmonary disease with acute exacerbation
0304	50	0	Antihistamines, hyposensitisation and allergic emergencies
J301	50	0.04	Allergic rhinitis due to pollen
0105/0302/ 0501/0504/ 0603/0802/ 1001	50	0.01	Chronic bowel disorders/Corticosteroids (respiratory)/ Antibacterial drugs/Antiprotozoal drugs/ Corticosteroids (endocrine)/Drugs affecting the immune response/ Drugs used in rheumatic diseases and gout

0301	51	0	Bronchodilators	J459	52	0	Asthma
0304	51	0	Antihistamines, hyposensitisation and allergic emergencies	0302	52	0	Corticosteroids (respiratory)
0302	51	0.45	Corticosteroids (respiratory)	0301	52	0	Bronchodilators
J441	51	0.99	Chronic obstructive pulmonary disease with acute exacerbation	0301	52	0	Bronchodilators
0501	51	0.05	Antibacterial drugs	0302	52	0.03	Corticosteroids (respiratory)
0304	51	0	Antihistamines, hyposensitisation and allergic emergencies	0403	52	0	Antidepressant drugs
0301	51	0	Bronchodilators	F329	52	0	Depressive episode
0105/0302	51	0	Chronic bowel disorders/Corticosteroids (respiratory)/	0301	52	0	Bronchodilators
/0501/0504			Antibacterial drugs/Antiprotozoal drugs/	0302	52	0	Corticosteroids (respiratory)
/0603/0802			Corticosteroids (endocrine)/Drugs affecting the immune response/	0302	52	0	Corticosteroids (respiratory)
/1001			Drugs used in rheumatic diseases and gout	0304	52	0	Antihistamines, hyposensitisation and allergic emergencies
0302	51	0	Corticosteroids (respiratory)	0301	52	0	Bronchodilators
0302	51	0	Corticosteroids (respiratory)	0302	52	0	Corticosteroids (respiratory)
0304	51	0	Antihistamines, hyposensitisation and allergic emergencies	0302	52	0	Corticosteroids (respiratory)
0301	51	0	Bronchodilators	0304	52	0.02	Antihistamines, hyposensitisation and allergic emergencies
0304	51	0.03	Antihistamines, hyposensitisation and allergic emergencies	0301	52	0.09	Bronchodilators
0301	51	0.01	Bronchodilators	0301	52	0	Bronchodilators
0302	51	0	Corticosteroids (respiratory)	0302	52	0.01	Corticosteroids (respiratory)
0301	51	0	Bronchodilators	0302	52	0	Corticosteroids (respiratory)
0304	51	0	Antihistamines, hyposensitisation and allergic emergencies	0301	52	0	Bronchodilators
0302	51	0	Corticosteroids (respiratory)	0501	52	0	Antibacterial drugs
0304	51	0	Antihistamines, hyposensitisation and allergic emergencies	J22	52	0	Acute lower respiratory infection
0302	51	0	Corticosteroids (respiratory)	0301	52	0	Bronchodilators
0304	51	0	Antihistamines, hyposensitisation and allergic emergencies	0302	52	0.04	Corticosteroids (respiratory)
0302	51	0	Corticosteroids (respiratory)	J40	52	0	Bronchitis
0301	51	0	Bronchodilators	0302	52	0	Corticosteroids (respiratory)
0302	51	0	Corticosteroids (respiratory)	0501	52	0	Antibacterial drugs
0301	51	0	Bronchodilators	0301	52	0	Bronchodilators
0302	51	0	Corticosteroids (respiratory)	0105/0302/	52	0	Chronic bowel disorders/Corticosteroids (respiratory)/
0301	51	0	Bronchodilators	0501/0504/			Antibacterial drugs/Antiprotozoal drugs/
0302	51	0	Corticosteroids (respiratory)	0603/0802/			Corticosteroids (endocrine)/Drugs affecting the immune response/
0301	51	0	Bronchodilators	1001			Drugs used in rheumatic diseases and gout
0302	51	0	Corticosteroids (respiratory)	0501	52	0	Antibacterial drugs
0301	51	0.44	Bronchodilators	0501	52	0	Antibacterial drugs
0501	51	0.2	Antibacterial drugs	0301	53	0.14	Bronchodilators
J441	51	0	Chronic obstructive pulmonary disease with acute exacerbation	0302	53	0	Corticosteroids (respiratory)
0301	51	0	Bronchodilators	0105/0302/	53	0	Chronic bowel disorders/Corticosteroids (respiratory)/
0302	51	0	Corticosteroids (respiratory)	0501/0504/			Antibacterial drugs/Antiprotozoal drugs/
0501	51	0.01	Antibacterial drugs	0603/0802/			Corticosteroids (endocrine)/Drugs affecting the immune response/
J029	51	0	Acute pharyngitis	1001			Drugs used in rheumatic diseases and gout
0301	51	0	Bronchodilators				
0302	51	0	Corticosteroids (respiratory)				
0301	51	0	Bronchodilators				
0302	51	0	Corticosteroids (respiratory)				
0301	52	0	Bronchodilators				
0302	52	0	Corticosteroids (respiratory)				

J441	53	1	Chronic obstructive pulmonary disease with acute exacerbation	J40	53	0	Bronchitis
0501	53	0	Antibacterial drugs	0301	53	0	Bronchodilators
0501	53	0	Antibacterial drugs	0501	53	0	Antibacterial drugs
0105/0302/	53	0	Chronic bowel disorders/Corticosteroids (respiratory)/	0105/0302/	53	0	Chronic bowel disorders/Corticosteroids (respiratory)/
0501/0504/			Antibacterial drugs/Antiprotozoal drugs/	0501/0504/			Antibacterial drugs/Antiprotozoal drugs/
0603/0802/			Corticosteroids (endocrine)/Drugs affecting the immune response/	0603/0802/			Corticosteroids (endocrine)/Drugs affecting the immune response/
1001			Drugs used in rheumatic diseases and gout	1001			Drugs used in rheumatic diseases and gout
0501	53	0	Antibacterial drugs	0501	53	0	Antibacterial drugs
0301	53	0.37	Bronchodilators	J441	53	0.01	Chronic obstructive pulmonary disease with acute exacerbation
0302	53	0	Corticosteroids (respiratory)	J22	54	0.22	Acute lower respiratory infection
J029	53	0.06	Acute bronchitis	0501	54	0	Antibacterial drugs
0501	53	0.01	Antibacterial drugs	0302	54	0	Corticosteroids (respiratory)
0301	53	0.01	Bronchodilators	0301	54	0.41	Bronchodilators
0302	53	0	Corticosteroids (respiratory)	J029	54	0	Acute pharyngitis
0304	53	0	Antihistamines, hyposensitisation and allergic emergencies	0501	54	0.41	Antibacterial drugs
0302	53	0	Corticosteroids (respiratory)	0501/1306	54	0.04	Antibacterial drugs/Acne and rosacea
0304	53	0	Antihistamines, hyposensitisation and allergic emergencies	I259	54	0.59	Chronic ischaemic heart disease
0301	53	0	Bronchodilators	0202	54	1	Diuretics
0304	53	0.01	Antihistamines, hyposensitisation and allergic emergencies	I219	54	1	Acute myocardial infarction
S526	53	0	Fracture of lower end of both ulna and radius	J449	54	1	Chronic obstructive pulmonary disease
0407	53	0	Analgesics	J459	54	1	Asthma
0301	53	0	Bronchodilators	0202	54	1	Diuretics
0302	53	0.01	Corticosteroids (respiratory)	0407/0407	54	0	Analgesics
0407/0407	53	0	Analgesics	0205	54	0	Anti-hypertensive drugs
0105/0302/	53	0	Chronic bowel disorders/Corticosteroids (respiratory)/	0301	54	0.02	Bronchodilators
0501/0504/			Antibacterial drugs/Antiprotozoal drugs/	0302	54	0	Corticosteroids (respiratory)
0603/0802/			Corticosteroids (endocrine)/Drugs affecting the immune response/	0301	54	1	Bronchodilators
1001			Drugs used in rheumatic diseases and gout	0202	54	0.48	Diuretics
J441	53	1	Chronic obstructive pulmonary disease with acute exacerbation	0302	54	0	Corticosteroids (respiratory)
0501	53	0.01	Antibacterial drugs	0301	54	0	Bronchodilators
0501	53	0	Antibacterial drugs	J22	54	0.97	Acute lower respiratory infection
J40	53	0	Bronchitis	0501	54	0	Antibacterial drugs
0501	53	0	Antibacterial drugs	0501	54	0	Antibacterial drugs
J029	53	0.07	Acute pharyngitis	0202	54	0	Diuretics
0501	53	0	Antibacterial drugs	0301	54	0	Bronchodilators
0302	53	0.02	Corticosteroids (respiratory)				
0105/0302/	53	0	Chronic bowel disorders/Corticosteroids (respiratory)/				
0501/0504/			Antibacterial drugs/Antiprotozoal drugs/				
0603/0802/			Corticosteroids (endocrine)/Drugs affecting the immune response/				
1001			Drugs used in rheumatic diseases and gout				